REPORT DOCUMENTATION PAGE

Form Approved
OMB No. 0704-0188

1. REPORT DATE *(DD-MM-YYYY)*	2. REPORT TYPE	3. DATES COVERED *(From - To)*
31-03-2004	Final	01-03-2002 - 31-03-2004

4. TITLE AND SUBTITLE
Optical Measurements of Ground Vibrations

5a. CONTRACT NUMBER

5b. GRANT NUMBER
N00014-02-1-0346

5c. PROGRAM ELEMENT NUMBER

6. AUTHOR(S)
James M. Sabatier
Andi G. Petculescu

5d. PROJECT NUMBER

5e. TASK NUMBER

5f. WORK UNIT NUMBER

7. PERFORMING ORGANIZATION NAME(S) AND ADDRESS(ES)
University of Mississippi
National Center for Physical Acoustics
P. O. Box 1848
University, MS 38677

8. PERFORMING ORGANIZATION REPORT NUMBER
JMS0304-2

9. SPONSORING/MONITORING AGENCY NAME(S) AND ADDRESS(ES)
Office of Naval Research Regional Office
100 Alabama Street SW Suite 4R15
Atlanta, GA 30303-3104

10. SPONSOR/MONITOR'S ACRONYM(S)

12. DISTRIBUTION/AVAILABILITY STATEMENT
APPROVED FOR PUBLIC RELEASE; DISTRIBUTION IS UNLIMITED.

13. SUPPLEMENTARY NOTES

14. ABSTRACT

The Office of Naval Research issued Grant N00014-02-1-0346 for Optical Measurements of Ground Vibrations to the National Center for Physical Acoustics at the University of Mississippi. The University of Mississippi is involved in an applied research program to develop an acoustic technique to detect buried landmines. In this technique, the ground is excited using acoustic or seismic sources which elicit resonance in buried mines. This resonance causes increased amplitude in the ground vibration over the buried object. The primary methods of measuring ground vibration involve laser Doppler vibrometry and tend to limit operational tempo due to long scanning times and be adversely affected by loose ground cover. Research has been performed to develop a Doppler acoustic technique for the measurement of ground vibration. Initial laboratory and field tests indicate this device has significant promise for overcoming the current limitations.

15. SUBJECT TERMS
Ultrasonic Doppler vibrometry, acoustic landmine detection, acoustic vibration sensing, landmine detection

16. SECURITY CLASSIFICATION OF:			17. LIMITATION OF ABSTRACT	18. NUMBER OF PAGES	19a. NAME OF RESPONSIBLE PERSON
a. REPORT	b. ABSTRACT	c. THIS PAGE			James M. Sabatier
U	U	U	A	39	19b. TELEPHONE NUMBER *(Include area code)* 662-915-5404

ACOUSTIC TECHNOLOGY FOR LANDMINE DETECTION

ANNUAL REPORT

GRANT NUMBER: N00014-02-1-0346

SUBMITTED TO:

OFFICE OF NAVAL RESEARCH
BALLSTON CENTRE TOWER ONE
800 NORTH QUINCY STREET
ARLINGTON, VA 22217-5660

by

James M. Sabatier
National Center for Physical Acoustics
University of Mississippi
University, MS 38677

NCPA Report JS0304-02

31 MARCH 2004

SECURITY CLASSIFICATION: UNCLASSIFIED

OPTICAL MEASUREMENTS OF GROUND VIBRATIONS
FINAL REPORT

0.0 ABSTRACT

The Office of Naval Research issued Grant N00014-02-1-0346 for Optical Measurements of Ground Vibrations to the National Center for Physical Acoustics at the University of Mississippi. The University of Mississippi is involved in an applied research program to develop an acoustic technique to detect buried landmines. In this technique, the ground is excited using acoustic or seismic sources which elicit resonance in buried mines. This resonance causes increased amplitude in the ground vibration over the buried object. The primary methods of measuring ground vibration involve laser Doppler vibrometry and tend to limit operational tempo due to long scanning times and be adversely affected by loose ground cover. Research has been performed to develop a Doppler acoustic technique for the measurement of ground vibration. Initial laboratory and field tests indicate this device has significant promise for overcoming the current limitations.

1.0 TABLE OF CONTENTS

2.0 INTRODUCTION

The proliferation of relatively cheap landmines in many of the world's conflicts has led to a critical situation. The current methods of locating landmines trigger on too many false alarms that must each be investigated before declaring and area to be clear of mines. Meanwhile, plastic landmines have been developed that cannot be detected using metal detectors. The confluence of these two factors has led the US military to seek accurate means of detection coupled with a low false alarm rate. Beginning in 1997, the US Army Night Vision and Electronic Sensors Directorate (NVESD) has issued a series of contracts to the University of Mississippi's National Center for Physical Acoustics (NCPA) to develop acoustic technique for locating buried landmines. The Office of Naval Research has also assumed a key role in this applied research program by providing grants for equipment, research into the causes and reduction techniques for false alarms, and research into alternative sensors.

Landmines are acoustically located by exciting the ground using sound waves. Differences in resonance cause the insonified ground to vibrate with greater amplitude over buried objects. The vibration is measured using a non-contact device and the signal is processed to produce an image of the buried landmine.

The NCPA has demonstrated the effectiveness of this technique in testing under varying conditions including temperate and desert conditions in numerous types of soil. These tests have included blind tests in which the testers did not know whether or not a section of ground contained a mine and have included both downward and forward-looking tests. The results of each test series clearly showed that the acoustic technique is a very accurate means for locating landmines with a low false alarm rate [1][2].

The non-contact devices currently used primarily focus on various applications of laser Doppler vibrometry and are limited scientifically by slow scanning times and difficulty in measurement of the ground under loose vegetation. From a life cycle cost standpoint, they are limited by their acquisition cost and sensitivity to ambient vibration.

To aid in overcoming these limitations, the University of Mississippi has conducted research on Doppler acoustic sensor.

3.0 METHODS, ASSUMPTIONS, PROCEDURES, RESULTS AND DISCUSSION

The University of Mississippi conducted research to systematically investigate the feasibility, capabilities, and limitations of an acoustic Doppler vibration measurement device. The methods, assumptions, procedures, and results are discussed in detail in Appendices A, B, C, and D, which are published reports of this work in peer-reviewed journals and mine detection related, non-peer-reviewed proceedings.

Based on the success of this project, continuing research regarding this device will be integrated into the Army's ongoing applied research program for acoustic mine detection.

4.0 REFERENCES

[1] J. M. Sabatier, "Acoustic Technology For Landmine Detection", Final Report, Contract Number: DAAB07-97-C-6040, NCPA Report JS0700-01, 1 February 2001, 66 pages.

[2] J. M. Sabatier, "Acoustic Technology For Landmine Detection", Final Report, Contract Number: DAAB15-00-C-1005, NCPA Report JS0303-01, 20 March 2003, 387 pages.

A feasibility study of an air-coupled acoustic sensor for measuring ground vibrations

Andi G. Petculescu, James M. Sabatier
National Center for Physical Acoustics, 1 Coliseum Drive, University MS 38677

Proc. SPIE Vol. 5089, p. 487-494, (2003).

ABSTRACT

Representative data pertaining to various critical aspects of air-coupled ultrasonic Doppler sensing of ground vibrations are presented. The behavior of an ultrasonic sensor is systematically compared with that of commercial laser vibrometers. The inherent drawbacks and advantages of both techniques are discussed and evaluated in systematic experiments. The experiments are designed so as to synthesize various scenarios that may be encountered in practice. Thus the vibration sensing capability of ultrasonic vibrometers is investigated in cases including flat and grass-covered surfaces, granular media, with and without ambient air motion. The work is supported by the Office of Naval Research.

1. INTRODUCTION

The objective of this study is to systematically investigate the operation of air-coupled ultrasonic vibrometers for measuring small ground vibrations. The work is motivated by the ongoing effort at the National Center for Physical Acoustics (NCPA) to develop alternative sensors for landmine detection. Among the pioneering work performed at NCPA in this field, laser Doppler vibrometry (LDV) used in conjunction with acoustic-to-seismic coupling has proven to be a reliable way to detect landmines [1,2,3,4]. A major source of signal degradation in the LDV technique consists of loss of useful optical power when probing grass-covered surfaces. An acoustic approach, on the other hand, is expected to be less sensitive given the relative ease of tuning the transmitter to frequencies able to penetrate grass or other scattering centers on the surface. Detailed engineering details involved in the development of an ultrasonic Doppler sensor capable of detecting a landmine in the presence of surface waves in compacted sand is given in Ref. 5.

An acoustic field incident on a vibrating surface is *not* a non-contact technique *per se*; the fluid that supports wave propagation acts as the coupling medium, in contact with both the sensor and the surface. In addition to the (surface-constrained) linear kinematic transformation represented by the Doppler effect[6,7,8], the acoustic energy radiated by the surface may couple nonlinearly with the probe field (mixing)[9,10,11]. However, the strength of this interaction depends primarily on medium nonlinearities. The nonlinear mixing increases with the interaction volume whereas the Doppler effect is restricted to the vibrating boundary. Piquette and Van Buren[9-11] argue that, in liquid media, a reduction of the ultrasonic probe power causes *commensurate* drops in the (linear) Doppler and nonlinear effects. However, these issues are beyond the scope of the present work.

2. METHODOLOGY

Consider a surface vibrating sinusoidally in the normal direction $\mathbf{n}_s$ with angular frequency Ω. Its instantaneous velocity is $\mathbf{V}(t) = \mathbf{n}_s u_s \cos \Omega t$, u_s being the magnitude. Let $\mathbf{k}$ and $\mathbf{q}$ be the incident and reflected wave vectors, respectively. The displacement amplitude is

$$\xi_s(t) = \frac{u_s}{\Omega} \sin \Omega t . \qquad (1)$$

Using the phase invariance under a linear coordinate transformation and the fact that frequency is the time-derivative of instantaneous phase, one obtains the change in frequency upon reflection from the oscillating boundary as

$$\omega_r(t) = \omega_i + (\mathbf{q} - \mathbf{k}) \cdot \mathbf{V}(t). \qquad (2)$$

Appendix A

The temporal phase of the reflected field is determined from the time integral of (2):

$$\Phi_r(t) = \omega_i t + (\mathbf{q} - \mathbf{k}) \cdot \mathbf{n}_s \, \xi_s(t). \tag{3}$$

Equations (2) and (3) represent the *instantaneous frequency* and *instantaneous phase*, respectively, of the angle modulated field. The received plane-wave pressure field is:

$$p_r(r,t) = |p_r| e^{i\mathbf{q}\cdot\mathbf{r}} e^{-i\left[\omega_i t + (\mathbf{q}-\mathbf{k})\mathbf{n}_s \frac{u_s}{\Omega} \sin \Omega t\right]}, \tag{4}$$

where $|p_r|$ is its magnitude. The right-hand exponent term in the brackets represents a sinusoidal modulation of the signal phase. The information pertaining to the surface vibration can be extracted by demodulation of the received signal.[12] In general terms, frequency or phase demodulation, generates a voltage proportional to the instantaneous frequency $\omega_i(t)$ or phase $\Phi_i(t)$, respectively. According to Equations (2) and (3), frequency demodulation yields a direct measure of the vibration *velocity* amplitude, while phase demodulation is directly related to the *displacement* amplitude.

In keeping with electronic communications theory, a *phase modulation index* is introduced as

$$\beta \equiv (\mathbf{q} - \mathbf{k}) \cdot \mathbf{n}_s \frac{u_s}{\Omega}. \tag{5}$$

Assuming $u_s << c_0$ (c_0 being the speed of sound in the medium), the modulation index β becomes[13]

$$\beta \approx \frac{2\omega_i}{c_0} \frac{u_s}{\Omega} \cos\theta = \frac{2\omega_i}{c_0} \xi_s \cos\theta. \tag{6}$$

$\xi_s \equiv u_s/\Omega$ denotes the displacement magnitude and θ is the incidence angle. Using the Bessel generating functions, Equation (4) becomes

$$p_r(r,t) = \sum_{n=-\infty}^{\infty} |p_r| J_n(\beta) e^{-i(\omega_i + n\Omega)t} e^{i\mathbf{q}\cdot\mathbf{r}}, \tag{7}$$

where J_n is the Bessel function of the first kind. Equation (7) is essential to investigating the operation of ultrasonic vibrometers. The energy in the received ultrasonic field is divided between the central "carrier" (n = 0) and an infinite number of symmetric sidebands, of frequencies $\omega_i \pm n\Omega$ and amplitudes $|p_r| J_n(\beta)$. The sidebands contain all the information pertinent to the surface vibration. For very small modulation indices, the only surviving orders in the Bessel series are n = 0, ±1. The Bessel functions satisfy $J_{-1}(\beta) = -J_1(\beta)$ and, given the small-argument behavior of Bessel functions, $J_0(\beta) \approx 1$ and $J_1(\beta) \approx \beta/2$. Thus the vibration sidebands are out of phase, with amplitudes (called *SB*, for simplicity) given by

$$SB \approx \pm |p_r| \frac{u_s}{\Omega} \frac{\omega_i}{c_0} \cos\theta. \tag{8}$$

Assuming weak dissipation, the magnitude of the received pressure is close to that of the incident field, $|p_r| \approx |p_i|$. From Equations (6)–(8) it is clear that the sensitivity can be increased if the vibration amplitude, probe amplitude and/or the probe frequency are increased.

Often the sensor is scanned at constant speed over the surface, as opposed to stop-and-stare operation. In many practical applications (such as measurement of soil vibrations), the surface is not always parallel to the scanning direction. This additional sensor-surface relative motion adds an extra frequency shift in Equation (2), proportional to the relative scanning velocity. Therefore, one must be careful to choose a scanning speed whose Doppler peak does not lie in the desired measurement bandwidth.

3. EXPERIMENTS

The experimental arrangement is shown in Figure 1. Two similar custom-made piezoelectric transducers (center frequency ≈ 120 kHz, bandwidth ≈ 10 kHz, total divergence ≈ 9°) acting as transmitter and receiver form the sensor. The modulated carrier is filtered and amplified by a low-noise preamplifier (SR560) and subsequently fed to a HP89410A vector signal analyzer, capable of real-time demodulation. An HP8904A signal generator supplies the transducer excitation for most measurements. Commercial shakers are used to excite the vibration of the probed surface. Two types of shakers are used: a clamped-plate type (AURA model AST-2B-4, f_{res} = 40 Hz) and a piston type (LDS model V203, broadband). The surface displacement amplitude is monitored with a Polytec PDV 100 laser Doppler vibrometer (LDV). In the next sections, the acronym UDV will be used for the ultrasonic Doppler vibrometer.

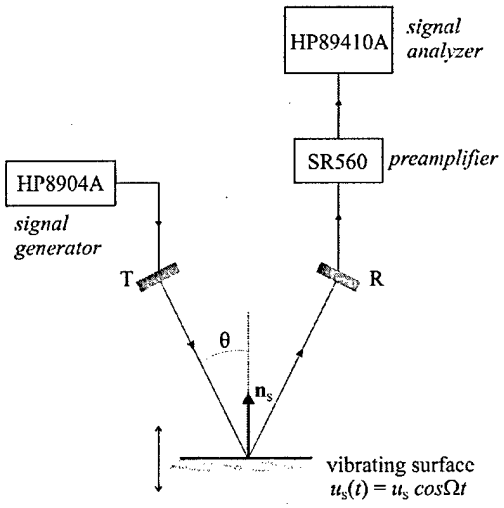

Figure 1: Experimental arrangement.

3.1 Spectral purity of the excitation signal

Figure 2 shows the effect of 60 Hz interference on the detected angle modulated carrier (using a rigidly mounted AURA shaker). In the particular case shown, the vibration frequency (150 Hz) is dangerously close to the ominous interference harmonics.

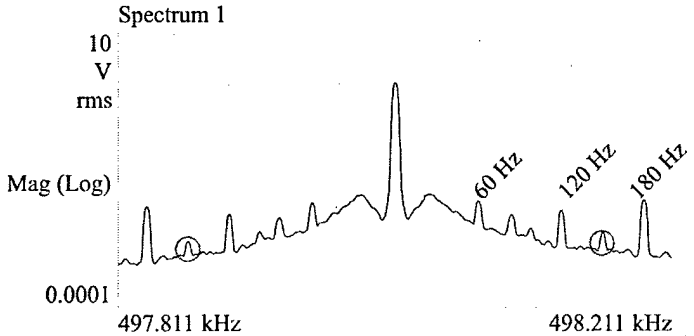

Figure 2: Example of data corrupted by 60 Hz harmonics and intermodulation products. The circles indicate the actual vibration sidebands; with the exception of the carrier, all the other signals are parasitic.

3.2 Sensor saturation

There are cases when increasing the probe power for greater sensitivity leads to a saturation regime of the transmitter. Such a case is shown in Figure 3, for a probe frequency of 498 kHz. V_{TX} is the transmitter excitation level. Both the upper and lower vibration sideband amplitudes are shown. No increase in sensitivity can be achieved past the point where the received carrier signal levels out.

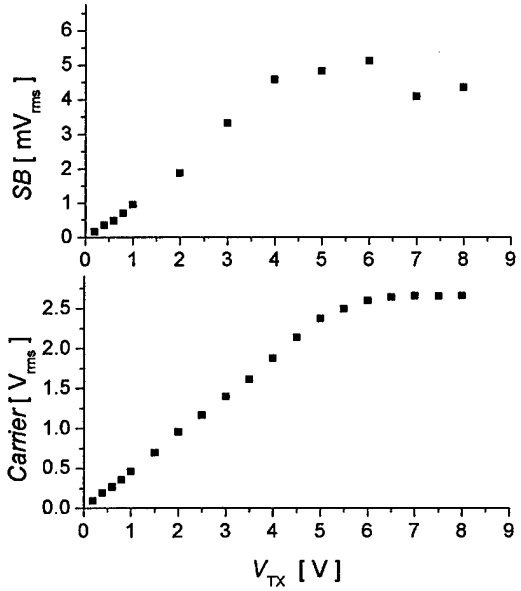

Figure 3: Example of sensor saturation. The sidebands give false information on the vibration displacement.

3.3 Linearity

The plots in Figure 4 are intended to assess the linearity of the measurement, using an AURA shaker. The sideband amplitude is plotted against the product of the shaker ("S") and transmitter ("TX") excitation levels $V_S V_{TX}$, for two cases: i) V_S is variable and V_{TX} is fixed (squares) and ii) V_{TX} is variable and V_S is fixed (circles). The three plots correspond to increasing the transmitter excitation to a point where it seems to saturate (V_{TX}=5V).

3.4 Probing sand vibrations

A more realistic scenario is presented in Figure 5. The AURA shaker was buried about 3cm in sand and exited at 150 Hz; the probe frequency was 120.4 kHz. The vibrations of the sand surface above the shaker were measured both with the UDV and the LDV. The aim of these types of investigations was to assess the ability of an ultrasonic sensor to accurately follow the "real" ground truth (as measured with an optical sensor). The example shown in the upper plots is unequivocal proof that the vibration information obtained ultrasonically has the same structure as that obtained with a commercial LDV. The white squares represent the sideband amplitudes obtained using a multi-carrier technique developed to increase sensitivity (which will be published separately). The energy dynamics between the carrier and the sidebands is evident in the lower graph showing the point-wise carrier values. The carrier behavior is interesting in itself since it could be used in conjunction with that of the sidebands to extract more information.

3.5 Effects of wind and grass

Commercial laser vibrometers may suffer from sensitivity limitations when used to probe grass-covered surfaces. Even in the absence of wind, a single blade of grass rooted in the vibrating surface often causes considerable loss of optical signal. Figure 6 shows a sequence of consecutive real-time LDV spectra illustrating the rising noise level due the loss of

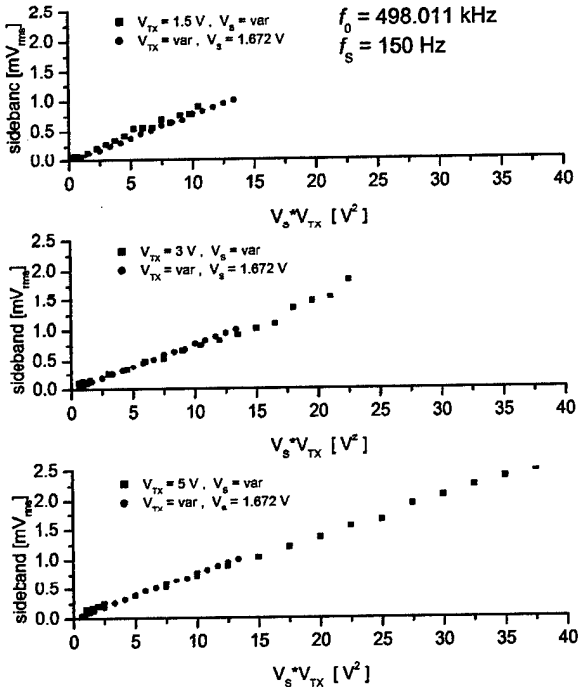

Figure 4: Sideband amplitude vs. excitation product on an AURA shaker oscillating at 150 Hz.

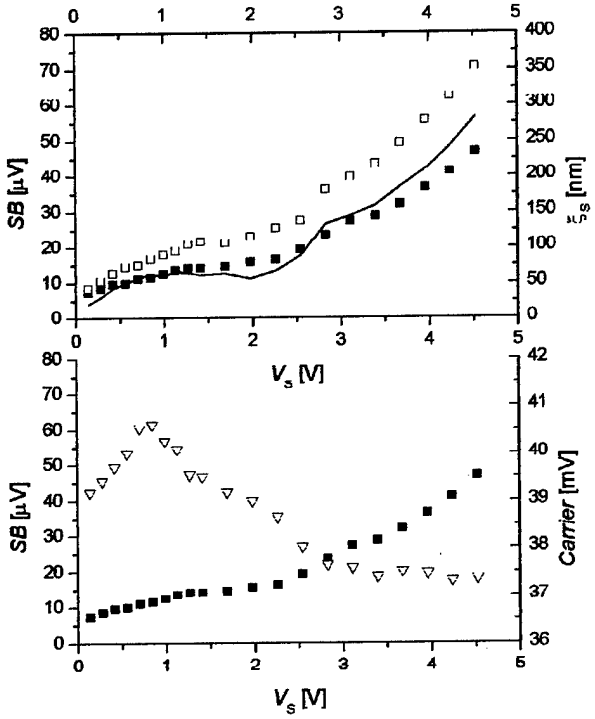

Figure 5: Comparison between UDV and LDV measuring sand vibrations above a buried shaker. Upper: black squares – sideband amplitude, white squares – multi-carrier sideband amplitude, solid line – surface displacement measured with LDV. Lower: triangles – carrier amplitude.

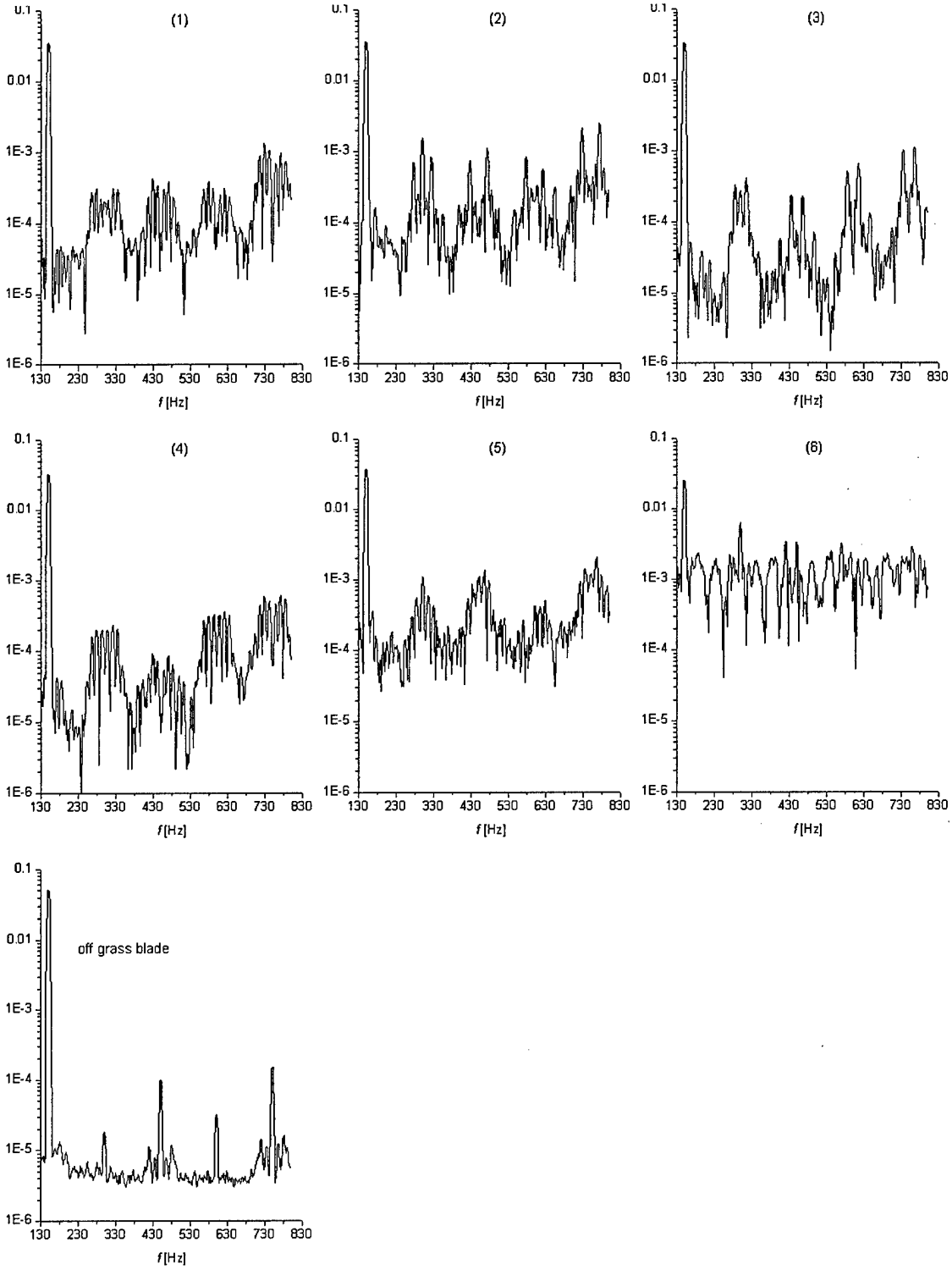

Figure 6: Illustration of loss of signal in an LDV when probing a vibrating blade of grass. The six–graph set shows a real-time sequence of the LDV signal on the grass blade; the last set member indicates almost total decoherence. The lowermost graph shows the clean LDV signal off the grass blade.

useful optical power when probing a blade of grass attached to the surface of a vibrating LDS shaker (150 Hz). The "clean" vibration signal obtained from the shaker surface directly is also shown, for comparison. The harmonics are due mostly to inherent shaker nonlinearities. Wind also affects the operation of ultrasonic sensors by scattering acoustic energy. When air motion is present, it induces a complex motion of the grass blades. In the laboratory, wind was simulated by compressed nitrogen jets. Figure 7 compares the effects of a weak jet blowing over a rooted-grass simulator (4mm wide paper strips inserted into closed-cell foam) on an optical (LDV) and ultrasonic (UDV) Doppler vibrometers. The spectra are averaged over the same time intervals. The complete loss of signal in the LDV is evident, as opposed to the UDV.

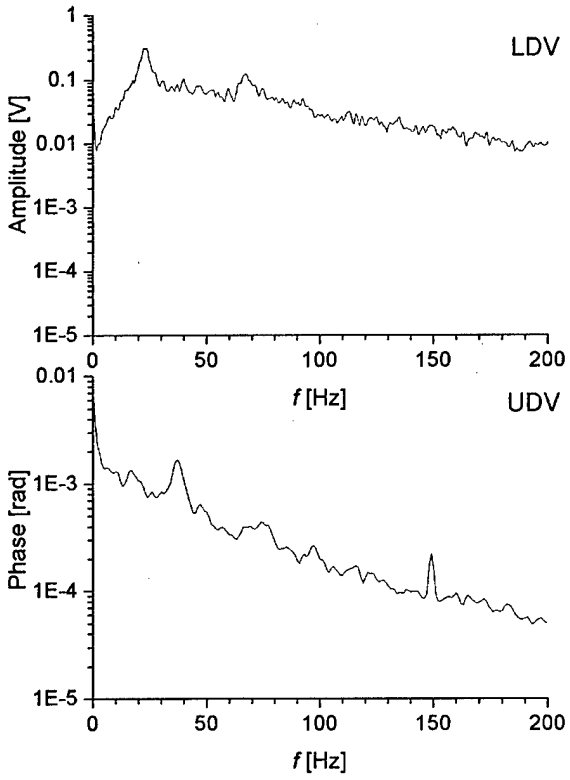

Figure 7: The LDV (upper) and UDV (lower) responses to a grassy surface vibrating at 150 Hz, in the presence of relatively weak air motion. For the UDV case, the demodulated phase is shown.

4. CONCLUSIONS

Several key aspects concerning the feasibility of ultrasonic probing of vibrating surfaces have been discussed. Among the factors that affect the operation of an UDV adversely is scattering by turbulent structures in the wind. This limitation can be overcome by using a shield around the sensor that prevents wind from entering the measurement region. Surface scattering issues can be addressed by operating at lower probe frequencies. It has been shown that wind is also detrimental to conventional optical vibrometers operating over vegetation-covered surfaces. By exploring ways to enhance the SNR by systematic physical studies and careful engineering, a UDV implementation can be developed, capable to yield reliable information where other sensors fail.

ACKNOWLEDGMENTS

Appendix A

This work is supported by a grant from the Office of Naval Research under Grant N00014-02-1-0346 Any opinions, findings and conclusions or recommendations expressed in this material are those of the authors and do not necessarily reflect the views of the Office of Naval Research.

REFERENCES

1. W. Patrick Arnott and J. M. Sabatier, "Laser-Doppler vibrometer measurements of acoustic to seismic coupling", Appl. Acoust. 30, 279-291 (1990).
2. N. Xiang and J. Sabatier, "Pre-differentiated M-sequences for laser-Doppler-based identification of vibrational systems", J. Acoust. Soc. Am. 106 (2), 2215 (A) (1999).
3. J. M. Sabatier and N. Xiang, "An Investigation of Acoustic-to-Seismic Coupling to Detect Buried Antitank Landmines", IEEE Transactions on Geoscience and Remote Sensing, 39, 6, 1146-1154, June (2001).
4. J. M. Sabatier and N. Xiang, "Laser-Doppler-based acoustic-to-seismic detection of buried mines", Proc. SPIE. 3710 215-222 (1999).
5. D. Fenneman, *An acoustic method for the detection of surface waves in sand*, Master's Thesis, Georgia Institute of Technology, July 2002.
6. D. Censor, "Harmonic and transient scattering from time-varying obstacles", J. Acoust. Soc. Am. 76 1527-1534 (1984).
7. D. Censor, "Scattering by time-varying obstacles", J. Sound Vib. 25, 101-110 (1972)
8. D. Censor, "Acoustical Doppler effect analysis – Is it a valid method?", J. Acoust. Soc. Am. 83, 1223-1230 (1988).
9. J. C. Piquette and A. L. Van Buren, "Comments on 'Harmonic and transient scattering from time-varying obstacles' ", J. Acoust. Soc. Am. 76, 1527-1534 (1984).
10. J. C. Piquette and A. L. Van Buren, "Some further remarks regarding scattering of an acoustic wave by a vibrating surface ", J. Acoust. Soc. Am. 80, 1533-1536 (1986).
11. J. C. Piquette and A. L. Van Buren, "Nonlinear scattering of acoustic waves by vibrating surfaces ", J. Acoust. Soc. Am. 76, 880-889 (1984).
12. B. P. Lathi, Modern Digital and AnalogCommunication Systems, Ch. 5, Oxford University, New York, 1998.
13. A. D. Pierce, Acoustics. An Introduction to Its Physical Principles and Applications, p.456, McGraw-Hill, New York, 1981.

REVIEW OF SCIENTIFIC INSTRUMENTS VOLUME 74, NUMBER 9 SEPTEMBER 2003

Signal-to-noise ratio improvement by sideband intermixing: Application to Doppler ultrasound vibrometry

Andi G. Petculescu[a] and James M. Sabatier
National Center for Physical Acoustics, 1 Coliseum Drive, University, Mississippi 38677

(Received 10 March 2003; accepted 15 June 2003)

A simple technique for improving the sensitivity of measuring devices based on angle modulation of a continuous-wave carrier is presented. The proposed approach involves the addition of a second carrier signal separated by twice the modulation frequency. In the Fourier domain, the upper sideband of the first carrier and the lower sideband of the second carrier intermix. By sweeping the relative phase between the two carriers, the magnitude of the resultant sideband can grow up to double the original value. In noisy environments, this effect can lead to an improvement of the signal-to-noise ratio. As a proof of concept, the technique is applied to a Doppler ultrasonic vibration sensor, with encouraging results. © *2003 American Institute of Physics.*
[DOI: 10.1063/1.1599070]

I. INTRODUCTION

Outside the world of electronic communications,[1] there are quite a few practical applications based on the frequency- or phase modulation of a carrier signal. As an example are motion and vibration Doppler sensors, whereby the phenomenon under investigation modulates the frequency or phase of a high-frequency incident wave. Depending on the applications, such sensors operate in the optical,[2,3] microwave,[4,5] and acoustic ranges.[6–9] Other applications are developed that implement fusion of several sensor types.[10,11] To the authors' knowledge, most continuous-wave sensors are based on the demodulation of a single modulated carrier. The present work lays the conceptual basis of a simple new technique that employs two tone-modulated carriers whose frequency separation is chosen such that a certain synchronicity condition is achieved.

II. THEORY

The case of two carrier signals of angular frequencies ω_1 and ω_2, angle modulated by a single tone with angular frequency Ω and phase modulation index β ($=\Delta\omega_{\max}/\Omega$, where $\Delta\omega_{\max}$ is the maximum frequency deviation[1]), is considered.

Assume the carriers have a relative phase difference φ and their frequencies are separated by twice the modulation frequency, i.e., $\omega_2=\omega_1+2\Omega$. If they are added together and sent through the channel, then the resultant signal is

$$\begin{aligned}\hat{p}(t)&=e^{-i(\omega_1 t+\beta\sin\Omega t)}+e^{-i(\omega_2 t+\beta\sin\Omega t+\varphi)}\\&=e^{-i(\omega_1 t+\beta\sin\Omega t)}+e^{-i(\omega_1 t+2\Omega t+\beta\sin\Omega t+\varphi)}\\&=2\cos(\Omega t+\varphi/2)e^{-i\varphi/2}e^{-i[(\omega_1+\Omega)t+\beta\sin\Omega t]}.\end{aligned}\tag{1}$$

Using the identity

$$e^{-iz\sin\theta}=\sum_{n=-\infty}^{\infty}J_n(z)e^{-in\theta}$$

in the rightmost exponential, one obtains

$$\begin{aligned}\hat{p}(t)=2\cos(\Omega t+\varphi/2)e^{-i\varphi/2}&\sum_{n=-\infty}^{\infty}J_n(\beta)\\&\times e^{-i[\omega_1 t+(n+1)\Omega t]}.\end{aligned}\tag{2}$$

The real part of Eq. (2) is

$$\begin{aligned}p(t)\equiv\mathrm{Re}[\hat{p}(t)]&=2\sum_{n=-\infty}^{\infty}J_n(\beta)\\&\times\cos[\omega_1 t+(n+1)\Omega t+\varphi/2]\cos(\Omega t+\varphi/2)\\&=\sum_{n=-\infty}^{\infty}J_n(\beta)\{\cos[\omega_1 t+(n+2)\Omega t+\varphi]\\&+\cos(\omega_1 t+n\Omega t)\}.\end{aligned}\tag{3}$$

Keeping only the orders $n=0,\pm1$ (thereby limiting the applicability of the method to small phase modulation indices β), rearranging in increasing frequency order, and keeping in mind that $\omega_2=\omega_1+2\Omega$, Eq. (3) becomes

$$\begin{aligned}p(t)\approx&-J_1(\beta)\cos(\omega_1-\Omega)t+J_0(\beta)\cos\omega_1 t\\&+2J_1(\beta)\sin[(\omega_1+\Omega)t+\varphi/2]\sin\varphi/2\\&+J_0(\beta)\cos\omega_2 t+J_1(\beta)\cos[(\omega_2+\Omega)t+\varphi].\end{aligned}\tag{4}$$

In the derivation of Eq. (4), the Bessel function property $J_{-1}(\beta)=-J_1(\beta)$ along with basic trigonometric relationships have been used. The $\omega_1-\Omega$ and $\omega_2+\Omega$ sidebands have constant magnitudes, equal to $J_1(\beta)$. The magnitude of the central term containing the resultant sideband oscillates between the limits $\pm2J_1(\beta)$, i.e., its magnitude can increase up to twice that of the individual sidebands. The first-order sidebands of a phase-modulated signal are π radians out-of-

[a]Author to whom correspondence should be addressed; electronic mail: apetcule@olemiss.edu

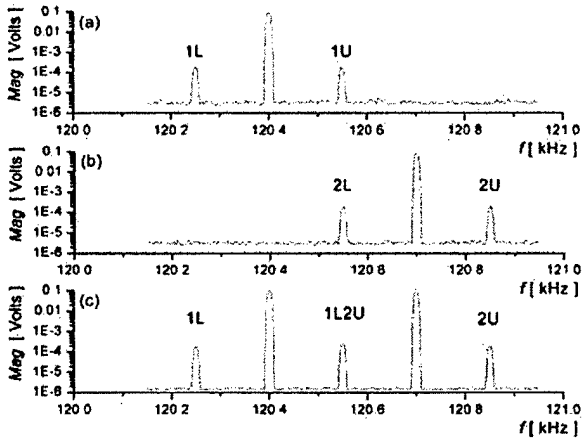

FIG. 1. Addition of two electronically frequency modulated carriers (time-averaged data): (a) carrier 1 only, (b) carrier 2 only, (c) carrier 1+carrier 2. The modulation frequency is 150 Hz. Note the logarithmic magnitude axis.

phase with each other; with a π-radian phase shift between the two carriers, the upper sideband of the low-frequency signal, and the lower sideband of the high-frequency signal will interfere constructively. This fact has potential use as a means to increase the signal-to-noise ratio in various applications.

III. EXPERIMENT

The following notations will be used: (i) when the two carriers are sent individually, 1L, 1U, 2L, and 2U denote the lower and upper sidebands of carrier 1 and carrier 2, respectively, and (ii) when the sum of the two carriers is sent, 1U 2L denotes the resultant sideband. A preliminary test was done using two carrier signals of 100 mV, each electronically frequency modulated with $f_{\text{mod}}=150$ Hz and a maximum deviation of 0.540 Hz. Two different signal generators had to be used for this purpose; additionally, the two modulated carriers were added by an in-house built summing amplifier. The function generators were referenced to a 10 MHz signal generated by the source of the spectrum analyzer. It is suspected that, despite this precaution, other phase/frequency shifts induced by mismatches in the electronics caused the overall phase of the resultant sideband (1U 2L) to change continuously, resulting in magnitude oscillations. The magnitude of the 1U 2L sideband oscillates between the noise floor and twice the magnitude of the other sidebands, which qualitatively corroborates Eq. (4). The time-averaged spectra are presented in Fig. 1.

In order to test its feasibility, the technique was applied to ultrasonic sensing of surface vibrations. A vibrating surface modulates the phase (or, equivalently, the frequency) of an incident acoustic probe field, giving rise to sidebands. The acronym UDV will be used for an ultrasonic Doppler vibrometer, throughout the article, A schematic diagram of the experimental arrangement is shown in Fig. 2. Two piezoelectric transducers (center frequency≈120 kHz, bandwidth≈10 kHz) acting as transmitter and receiver form the sensor. The multichannel HP8904A signal generator capable of signal summation supplies the excitation for the two primary signals, at frequencies equal to 120.4 kHz (carrier 1) and 120.7

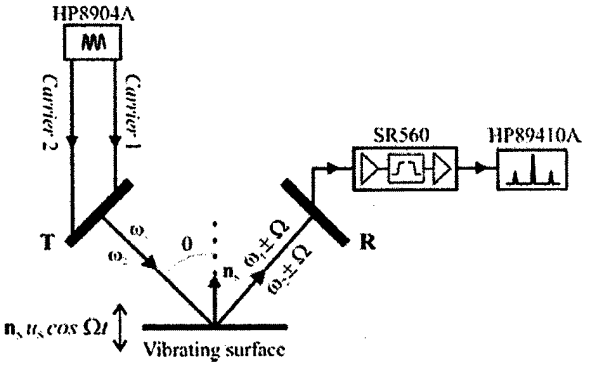

FIG. 2. Schematic diagram of the UDV arrangement. T and R denote the ultrasonic transmitter and receiver, respectively.

kHz (carrier 2). The modulated carriers are filtered and amplified 500 times by a low-noise preamplifier (SR560) and subsequently fed to an HP89410A vector signal analyzer. The gain was chosen such that the signal magnitude is close to that from the electronic modulation case of Fig. 1. Commercial shakers are used to excite the vibration of the probed surfaces; the velocity of the surface is $\mathbf{V}(t)=\mathbf{n}_s u_s \cos \Omega t$, where u_S is the magnitude and $\mathbf{n}_S$ is the unit vector normal to the surface. Two types of shakers are used: a clamped-plate type (AURA model AST-2B-4, $f_{\text{res}}=40$ Hz and a piston type (LDS model V203, broadband).

The data graphs in the next paragraphs contain information from time-averaged spectra of the detected ultrasonic signal. The first experiment involves probing an Al plate vibrating at $\Omega=150$ Hz. Figures 3(a) and 3(b) shows the UDV output when the two carrier frequencies are launched separately. Figure 3(c) represents an instance of the output when the two signals are summed and sent to the transmitter. Figure 4 reveals the excursion of the resultant sideband magnitude when carrier 2 is phase shifted in 10° increments, plotted together with the behavior of the other two sidebands. The inequality of the individual sidebands is most probably due to a misalignment of the sensor surface and/or to shaker nonlinearities. Nonetheless, this fact does not affect the over-

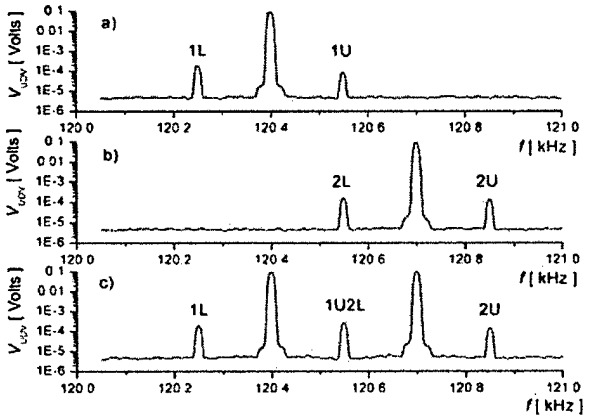

FIG. 3. Time-averaged spectra of the UDV output: (a) carrier 1 only, (b) carrier 2 only, (c) carrier 1+carrier 2. The modulation frequency is 150 Hz. Note the logarithmic magnitude axis.

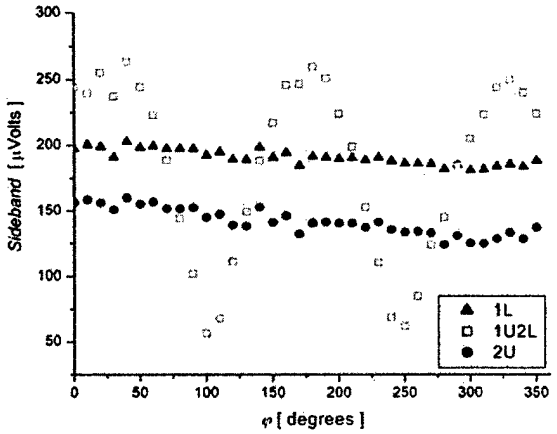

FIG. 4. UDV measurements on a surface vibrating at 150 Hz. Variation of the sideband magnitudes with the relative phase of the carriers. Note the difference between the maxima of the resultant sideband (1U 2L) and the unaffected sidebands.

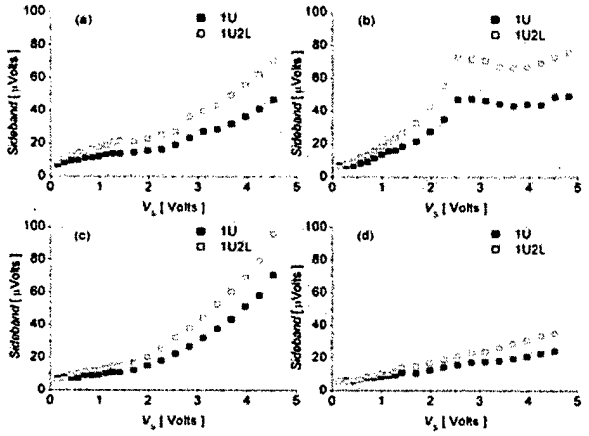

FIG. 5. Comparison between one-carrier and two-carrier operation of the UDV on a sand surface excited by an AURA shaker at 150 Hz. (a), (b) shaker buried ~3 cm below the surface, (c) shaker surface flush with sand surface, (d) shaker on lead bricks. V_s is the shaker excitation voltage.

all outcome (the authors have checked its consistency in several configurations with slightly different sideband ratios). Moreover, it acts to strengthen the case for real-life scenarios that may involve using ultrasonic sensors to measure complex surface vibrations. It is interesting to note the fact that the method basically uses the "interaction" of the 1U and 2L sidebands. In a purely conjectural context, analyzing the UDV operation from a kinematic, Doppler-effect angle, the upper and lower sidebands are produced by the surface going up and down, or *vice versa*. Thus, the 1U and 2L sidebands correspond to opposite surface "states," each probed by a different carrier wave vector.

Next, the two-carrier technique was applied to the ultrasonic sensing of vibrations of a rough, granular surface (sand). In this case, the AURA shaker was used and the UDV was positioned directly above it. The shaker excitation V_S was increased gradually and the UDV signal was recorded for each value. Figure 5 shows parallel plots of the averaged magnitudes of the upper sideband produced when carrier 1 alone is present and of the resultant sideband generated in the presence of carrier 1+carrier 2. The four graphs correspond to the case when the shaker is completely buried (a),(b), partially buried, with the surface flush with the sand surface (c), and not buried, resting on lead bricks (d). The improvement in sensitivity at the resultant sideband is evident.

ACKNOWLEDGMENT

The work was funded by a Grant from the Office of Naval Research.

[1] B. P. Lathi, *Modern Digital and Analog Communication Systems* (Oxford University Press, New York, 1998), Chap. 5.
[2] C. B. Scruby and L. E. Drain, *Laser Ultrasonics. Techniques and Applications* (Adam Hilger, Bristol, 1990), pp. 89–97.
[3] W. Patrick Arnott and J. M. Sabatier, Appl. Acoust. **30**, 279 (1990).
[4] J. S. Martin *et al.*, Proc. SPIE **4742**, 606 (2002).
[5] M. I. Skolnik, *Introduction to Radar Systems* (McGraw-Hill, New York, 1962).
[6] A. D. Pierce, *Acoustics: An Introduction to its Physical Principles and Applications* (McGraw-Hill, New York, 1981), p. 456.
[7] C. Baudet, O. Michel, and W. J. Williams, Physica D **128**, 1 (1999).
[8] D. Royer and O. Casula, Appl. Phys. Lett. **67**, 3248 (1995).
[9] A. G. Petculescu and J. M. Sabatier, J. Acoust. Soc. Am. (submitted).
[10] H. Russer and V. Magori, Eurosensors XIV, 28–30 August 2000, Copenhagen (available online at www.unibw-muenchen.de/campus/ET8/et82/Mitarb/HR/euro00_abs.pdf).
[11] W. R. Scott, Jr., C. Schroeder, and J. S. Martin, Proc. SPIE **3392**, 176 (1998).

Appendix C

Doppler Ultrasound Techniques for Landmine Detection

Andi G. Petculescu, James M. Sabatier
National Center for Physical Acoustics, 1 Coliseum Drive, University MS 38677

Proc. SPIE, (2004).

ABSTRACT

The paper presents measurements taken with a scanning ultrasonic Doppler vibrometer on a landmine buried separately in sand and in grass-covered soil. The signal obtained with a laser Doppler vibrometer experiences a large variability that is due to loss of spatial coherence upon scattering from moving grass blades. Ultrasonic sensing is not affected by this limitation since the acoustic speckle is much larger than its optical counterpart. Moreover, the slightest hint of air motion enhances the motion of the grass blades, which adds to the optical decoherence and subsequent loss of useful signal. It is shown also that the ultrasonic system has no problem penetrating the layer of grass and detecting the location of the buried target excited by a mechanical shaker.

Keywords: landmine detection, ultrasonic vibrometry, Doppler sensors

1. INTRODUCTION

The objective of this study is to investigate the potential application of an air-coupled Doppler ultrasonic sensor to the detection of buried landmines. Laser Doppler vibrometry (LDV) has proven to be a reliable way to detect resonance-excited landmines[1,2,3,4]. The LDV signal obtained from a grass-covered surface is affected by loss of optical power due to the very small speckle size. An acoustic approach, on the other hand, is expected to be less sensitive given the relative ease of tuning the transmitter to frequencies able to penetrate grass or other scattering centers on the surface. Also, air-coupled ultrasonics is able to provide the same range of wavelengths as microwave Doppler radar (MDR) does,[5] at frequencies several orders of magnitude smaller. Beside costs, this precludes the limitations associated with GHz electronics and signal processing. Detailed engineering details involved in the development of an ultrasonic Doppler sensor capable of detecting a landmine in the presence of surface waves in compacted sand is given in Ref. 6.

2. METHODOLOGY

The phenomenology of the ultrasonic Doppler technique is described in detail in Ref. 7. Consider a surface vibrating sinusoidally in the normal direction $\mathbf{n}_s$ with angular frequency Ω. Its instantaneous velocity is $\mathbf{V}(t) = \mathbf{n}_s u_s \cos\Omega t$, u_s being the magnitude. The received Doppler-shifted plane-wave pressure field is:

$$p_r(r,t) = |p_r| e^{i\mathbf{q}\cdot\mathbf{r}} e^{-i\left[\omega_i t + (\mathbf{q}-\mathbf{k})\mathbf{n}_s \frac{u_s}{\Omega} \sin\Omega t\right]}, \qquad (1)$$

where $|p_r|$ is its magnitude, ω_i is the incident acoustic frequency, $\mathbf{k}$ and $\mathbf{q}$ are the incident and reflected wave vectors, respectively. The right-hand exponent term in the brackets represents a sinusoidal modulation of the signal phase. The information pertaining to the surface vibration can be extracted by demodulation of the received signal.[8] In general terms, frequency or phase demodulation, generates a voltage proportional to the instantaneous frequency or phase, respectively. Frequency demodulation yields a direct measure of the vibration *velocity* amplitude, while phase demodulation is directly related to the *displacement* amplitude.

In keeping with electronic communications theory, the *phase modulation index* is, assuming $u_s \ll c_0$ (c_0 being the speed of sound in the medium),[9]

$$\beta \approx \frac{2\omega_i}{c_0}\frac{u_s}{\Omega}\cos\theta = \frac{2\omega_i}{c_0}\xi_s \cos\theta . \qquad (2)$$

$\xi_s \equiv u_s/\Omega$ denotes the displacement magnitude and θ is the incidence angle. Using the Bessel generating functions, Equation (1) becomes

$$p_r(r,t) = \sum_{n=-\infty}^{\infty} |p_r| J_n(\beta) e^{-i(\omega_i + n\Omega)t} e^{i\mathbf{q}\cdot\mathbf{r}}, \qquad (3)$$

where J_n is the Bessel function of the first kind. Equation (3) is essential to investigating the operation of ultrasonic vibrometers. The energy in the received ultrasonic field is divided between the central "carrier" (n = 0) and an infinite number of symmetric sidebands of frequencies $\omega_i \pm n\Omega$ and amplitudes $|p_r| J_n(\beta)$. The sidebands contain all the information pertinent to the surface vibration. For very small modulation indices, the only surviving orders in the Bessel series are n = 0, ±1. The Bessel functions satisfy $J_{-1}(\beta) = -J_1(\beta)$ and, given the small-argument behavior of Bessel functions, $J_0(\beta) \approx 1$ and $J_1(\beta) \approx \beta/2$. Thus the vibration sidebands are out of phase, with amplitudes (called *SB*, for simplicity) given by

$$SB \approx \pm |p_r| \frac{u_s}{\Omega} \frac{\omega_i}{c_0} \cos\theta . \qquad (4)$$

Assuming weak dissipation, the magnitude of the received pressure is close to that of the incident field, $|p_r| \approx |p_i|$.

3. EXPERIMENTS

3.1 Apparatus

The experimental arrangement is shown in Figure 1. Two similar Polaroid solid dielectric transducers (center frequency ≈ 50 kHz) acting as transmitter and receiver form the sensor. The modulated carrier is filtered and amplified by a low-noise preamplifier (SR560) and subsequently fed to a HP89410A vector signal analyzer, capable of real-time demodulation. An HP8904A signal generator supplies the transducer excitation for most measurements. The function generator can output two phase-controlled continuous-wave carriers. Two types of shakers are used to excite the vibration of the probed surface: a commercial clamped-plate type (AURA model AST-2B-4, f_{res} = 40 Hz) and, in the second part of the measurements, a custom-made push-pull shaker, specially designed to efficiently generate ground vibrations at long distances. The surface displacement amplitude is monitored with a Polytec PDV 100 laser Doppler vibrometer (LDV). In the next sections, the acronym UDV will be used for the ultrasonic Doppler vibrometer.

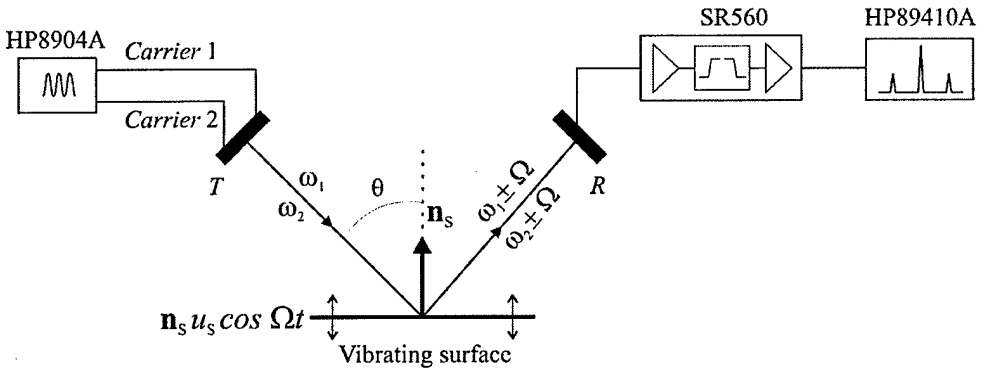

Figure 1. Experimental arrangement.

3.2 Effects of grass and wind

Commercial laser vibrometers suffer from sensitivity limitations when used to probe grass-covered surfaces. Even in the absence of wind, a single blade of grass rooted in the vibrating surface often causes considerable loss of optical signal. Figure 2 of Ref. 7 shows a sequence of consecutive real-time LDV spectra illustrating the loss of useful optical power when probing a blade of grass attached to the surface of a vibrating LDS shaker (150 Hz). Figure 2a shows how the LDV signal loses strength, contrary to the UDV, when probing a bed of pine needles vibrating at 150 Hz. In addition to this, very weak air motion adds a complex 3-component motion to the vibration of the grass blades that worsens the LDV signal loss, as opposed to the UDV (Figure 2b).

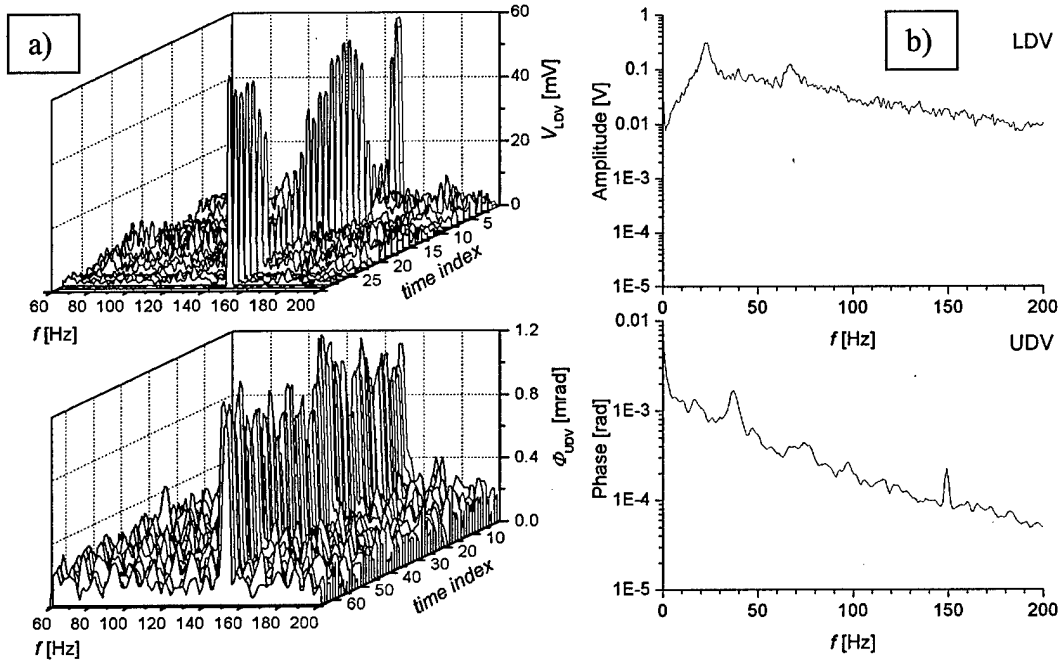

Figure 2. a) LDV (upper) and UDV (lower) signal variability from a vibrating bed of pine needles (150 Hz). b) The LDV (upper) and UDV (lower) responses to a grassy surface vibrating at 150 Hz, in the presence of very weak air motion that enhances motion of grass blades. For the UDV case, the demodulated phase is shown.

3.3 Ultrasonic Doppler sensing of a buried landmine

The first set of data was collected in the laboratory, in a large sand-filled box. An M15 landmine was buried 3 inches in sand. The elevation of the ultrasonic sensing head was 40 cm above the sand surface. The excitation was provided by the AURA shaker at 155 Hz, buried approximately 1 in below the surface, situated 75 cm away from the landmine. The sandbox dimensions were 1m x 2m, which precluded free-field conditions. Figure 3 shows the sandbox measurements. It has been found that the sensitivity of a continuous-wave Doppler vibrometer can be boosted by sending two carriers separated by twice the vibration (modulation) frequency.[10] When this condition is met, the received spectrum contains, besides the carriers, two "lateral" sidebands and one "mixed-state" sideband of twice the amplitude of the single-carrier case. A scan without the landmine was performed initially across the width of the box, in order to determine the "cavity" background mode at 155 Hz (solid line). Then the landmine was buried, and two scans were done: one with a single 50 kHz carrier (dotted line), and the other with two carriers at 50 kHz and 50.310 kHz (i.e. 50 kHz + 2 x 0.155 kHz) – dashed line. The landmine was located approximately between the 12 in and 24.5 in scan positions; the pressure plate was placed between the 15 in and 21 in positions. It is important to note that the ratio between the low-frequency wavelength (approx. 2 meters) and the other characteristic lengths (box width, landmine-shaker distance etc.), renders sensing of the landmine response *alone* impossible; the data shows the combined effects of the landmine response, on the one hand, and of the sandbox geometry on the other hand. What is essential, though, is that the 40-cm standoff ultrasonic sensor was able to readily detect the presence of the excited landmine buried inside the sand-filled "cavity".

The second experiment consisted of trying the ultrasonic vibrometer outdoors, on the same landmine, buried under almost 4 inches of grass-covered soil. As before, the sensing head was situated 40 cm above the ground surface; it was excited with 155 Hz in continuous-wave mode. This time, the free-field conditions were better approximated; also, AURA shaker was replaced by the in-house-built much more efficient push-pull shaker situated 3 meters away from the buried landmine. The results are presented in Figure 4. Starting from the right-hand side of the plot, the scan positions between 33 in and 23 in are off the target, while those from 23 in to almost 8 in are above the landmine (the point at 20.5 inches may contain an overload). The point here is that the UDV successfully "sees through" the dense grass; the speckle is much larger than in the optical case, due to the large discrepancy in the probing wavelengths.

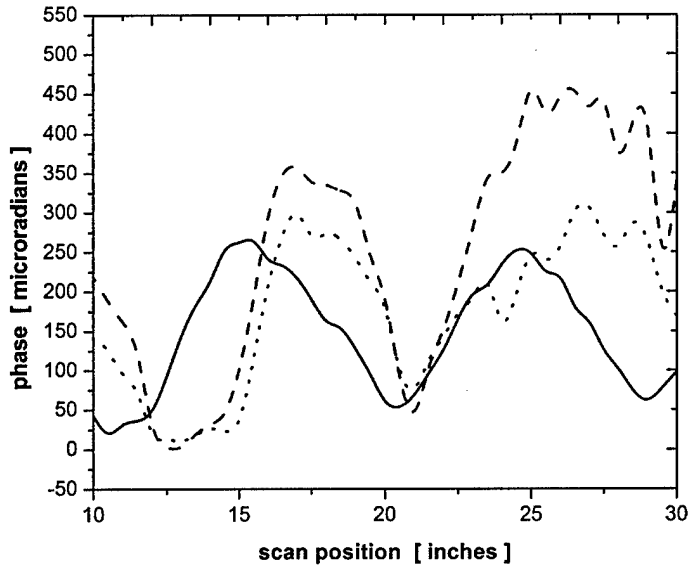

Figure 3. Landmine buried in sandbox. Solid = mine-free box mode; dotted = one-carrier operation; dashed = two-carrier operation. The pressure plate of the landmine was located approximately between the 15 and 21 in positions.

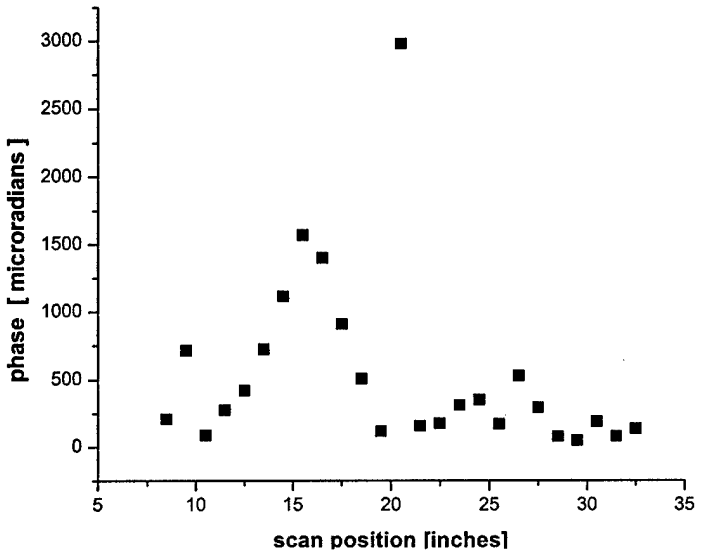

Figure 4. Scan across a landmine buried outdoors, under 4 inches of grass-covered soil.

4. CONCLUSIONS

It has been shown beyond the shadow of a doubt that ultrasounds can efficiently penetrate a dense layer of grass (or other low-lying vegetation) rooted in vibrating soil. Thus, an ultrasonic approach can either complement or replace optical sensors when probing vibrations of grass-covered surfaces. Signal degradation due to wind can be overcome by using a shield around the sensor that prevents wind from entering the measurement region. By exploring ways to enhance the SNR by systematic physical studies and careful engineering, a UDV implementation can be developed, capable to yield reliable information where other sensors fail.

5. ACKNOWLEDGEMENTS

This work was sponsored by the Office of Naval Research under Grant N00014-02-1-0346. Any opinions, findings, and conclusions or recommendations expressed in this material are those of the author(s) and do not necessarily reflect the views of the Office of Naval Research.

REFERENCES

1. W. Patrick Arnott and J. M. Sabatier, "Laser-Doppler vibrometer measurements of acoustic to seismic coupling", Appl. Acoust. 30, 279-291 (1990).
2. N. Xiang and J. Sabatier, "Pre-differentiated M-sequences for laser-Doppler-based identification of vibrational systems", J. Acoust. Soc. Am. 106 (2), 2215 (A) (1999).
3. J. M. Sabatier and N. Xiang, "An Investigation of Acoustic-to-Seismic Coupling to Detect Buried Antitank Landmines", IEEE Transactions on Geoscience and Remote Sensing, 39, 6, 1146-1154, June (2001).
4. J. M. Sabatier and N. Xiang, "Laser-Doppler-based acoustic-to-seismic detection of buried mines", Proc. SPIE. 3710 215-222 (1999).
5. W. R. Scott, Jr., C. Schroeder, and J. S. Martin, "An acousto-electromagnetic sensor for locating land mines", Proc. SPIE **3392**, *Detection and Remediation Technologies for Mines and Minelike Targets III*, 176-186, April 1998
6. D. Fenneman, *An acoustic method for the detection of surface waves in sand*, Master's Thesis, Georgia Institute of Technology, July 2002.
[7] A. G. Petculescu and J. M. Sabatier, "Feasibility study of an air-coupled acoustic sensor for measuring small vibrations", SPIE Aerosense 2003, Orlando, FL, April 2003
8. B. P. Lathi, Modern Digital and Analog Communication Systems, Ch. 5, Oxford University, New York, 1998.
9. A. D. Pierce, Acoustics. An Introduction to Its Physical Principles and Applications, p.456, McGraw-Hill, New York, 1981.
[10] A. G. Petculescu and J. M. Sabatier, "Signal-to-noise ratio improvement by sideband intermixing: Application to Doppler ultrasound vibrometry", Rev. Sci. Instrum. 74 (9), 4191-4193.

Air-coupled ultrasonic sensing of grass-covered vibrating surfaces; qualitative comparisons with laser Doppler vibrometry

J. Acoust. Soc. Am., 115 (4), April (2004).

Andi. G. Petculescu[(a)] and James. M. Sabatier

National Center for Physical Acoustics

1 Coliseum Drive, University, MS 38677

[(a)] e-mail: apetcule@olemiss.edu

Abstract

The paper addresses several sensitive issues concerning the use of air-coupled ultrasound to probe small vibrations of surfaces covered with low-lying vegetation such as grass. The operation of the ultrasonic sensor is compared to that of a laser Doppler vibrometer, in various contexts. It is shown that ambient air motion affects either system, albeit differently. As air speed increases, the acoustic sensor detects a progressively richer turbulent spectrum, which reduces its sensitivity. In turn, optical sensors are prone to tremendous signal losses when probing moving vegetation, due to randomly varying speckle patterns.
The work was supported by the Office of Naval Research.

PACS numbers: 43.35.Yb, 43.28.Gq

I. INTRODUCTION

Laser Doppler vibrometry (LDV) used in conjunction with acoustic-to-seismic coupling[1,2,3] has proven to be a reliable way to detect compliant and rigid buried objects.[4,5,6,7] Another technique based on the Doppler effect employs microwave Doppler radar (MDR).[8] Some applications require the use of arrays of a large number of sensors; as a result, the costs associated with implementing LDV or MDR systems become substantial. A major source of signal degradation in the LDV technique consists of loss of useful optical power when probing grass-covered surfaces. An acoustic approach, on the other hand, is expected to be less sensitive given the relative ease of tuning the transmitter to frequencies able to penetrate grass or other scattering centers on the surface. Also, air-coupled ultrasonics is able to provide the same range of wavelengths as MDR does, at frequencies several orders of magnitude smaller. Beside costs, this precludes the limitations associated with GHz electronics and signal processing. Several works have tackled the development of air-coupled ultrasonic vibration sensors to detect targets buried in sand in the presence of seismic surface waves[9,10]; however, to the best of the authors' knowledge, the influence of ambient air motion on ultrasonic sensor operation, as well as a direct comparison with optical sensors has not been addressed, in the context of Doppler vibrometry.

Ultrasonic Doppler sensors can be used in tandem with microwave radar, through phase coincidence. This concept explores the fact that the Doppler shifts generated by a target on the two types of sensors are coherent, despite external degrading factors which affect them differently.[11,12]

An acoustic field incident on a vibrating surface is *not* a non-contact technique *per se*; the fluid that supports wave propagation acts as the coupling medium, in contact with both the sensor and the surface. In addition to the (surface-constrained) linear kinematic transformation represented by the Doppler effect, the acoustic energy radiated by the surface may couple nonlinearly with the probe field (mixing). However, the strength of this interaction depends primarily on medium nonlinearities. The nonlinear mixing increases with the interaction volume whereas the Doppler effect is restricted to the vibrating boundary.[13] Casula and Royer[14] and Royer and Casula[15] describe the operation of a water-coupled,

normal-incidence, focused-ultrasound technique for measuring surface velocity transients. They show that, for water, the parametric interaction dominates after several surface vibration wavelengths. Barriere and Royer[16] use parametric interactions to measure the nonlinearity parameter of water and ethanol; they also develop a theoretical model of the diffraction effects on parametric interactions.

The main phenomenology of practical acoustic vibration sensors has been investigated thoroughly by various authors[17,18,19] and has made the subject of patented systems.[20] It has also been the center of much debate. For instance, two contending sides were Censor[21,22,23], and Piquette and Van Buren[24,25,26]. Censor tackles the problem kinematically, expressing the linearized wave equation via a Galilean coordinate transformation, within the quasistatic approximation (slow surface oscillation); this approach embodies the pure Doppler effect. In Ref. 23, Censor considers the effects of surface *and* medium motion, within the linear approximation. He argues that, in order for mass continuity to be observed, both cases must be included in the problem. Piquette and Van Buren embrace this idea for water as the propagation medium. They contend that, while laser vibrometers are based on the pure Doppler effect, since the governing (Maxwell's) equations are inherently linear, the acoustic case is inherently nonlinear due to the nature of the Navier-Stokes equation and should be treated as such. Moreover, they argue that, in liquid media, a reduction of the ultrasonic probe power causes commensurate drops in the (linear) Doppler and the nonlinear parametric effects. Due to the scope of the present work, these views will not be discussed further.

This work is motivated by the ongoing effort to develop alternatives to optical sensors for measuring vibrations of rough surfaces such as soils and sands through overlying vegetation (grass, leaves etc.). Through a series of comparative experiments, the authors present cases where ultrasonic sensors can be advantageous over laser vibrometers.

II. DOPPLER VIBROMETRY AND ANGLE MODULATION

In this section, the operation of an acoustic vibration sensor is described, based solely upon simple kinematic arguments. The line of thought is constructed in such a manner as to provide a connection

with experimental data. It is by no means intended as a thorough study of ultrasound Doppler sensors; see, for instance the referenced works by Censor and Piquette and Van Buren for attempts to quantify the phenomenology involved. Nevertheless, Censor's solution of the linearized wave equation (Ref. 23) yields results that reduce to those derived at the end of this section.

Consider a plane wave emitted by a transmitter in the laboratory system *S*, reflected by a target moving at constant velocity **V** (system S'), and detected back in *S*. If **k** and **q** are the incident (i) and reflected (r) wave-vectors, respectively, the frequency detected by the receiver in *S* is given by: [27]

$$\omega_r = \omega_i + (\mathbf{q} - \mathbf{k}) \cdot \mathbf{V} . \qquad (1)$$

The quantity $\Delta\omega_D \equiv (\mathbf{q} - \mathbf{k}) \cdot \mathbf{V}$ is the Doppler shift. Equivalently, Equation (1) states that during a small time interval d*t*, the phase of the incident field is changed, upon reflection, by the amount $(\mathbf{q} - \mathbf{k}) \cdot \mathbf{V} dt$.

In the case of Doppler vibration sensors, the "target" velocity is time-dependent. Consider a surface vibrating sinusoidally in the normal direction $\mathbf{n}_s$ with angular frequency Ω and instantaneous velocity $\mathbf{V}(t) = \mathbf{n}_s u_s \cos \Omega t$, u_s being the velocity amplitude (Figure 1). The instantaneous displacement of the surface is $\xi_s(t) = \mathbf{n}_s (u_s / \Omega) \sin \Omega t$.

Although the present study considers the simple bistatic geometry shown in Figure 1, it is useful to note the general character of the displacement amplitude $\xi_S(t)$: beside the case of translation of the surface parallel to itself, it can also represent tilt or rocking motion. The change in frequency upon reflection from the oscillating boundary is

$$\omega_r(t) = \omega_i + (\mathbf{q} - \mathbf{k}) \cdot \mathbf{V}(t) . \qquad (2)$$

The temporal phase of the reflected field is determined from the time integral of Equation (2):

$$\Phi_r(t) = \omega_i t + (\mathbf{q}-\mathbf{k})\cdot\int_0^t \mathbf{V}(\tau)\mathrm{d}\tau$$

$$= \omega_i t + (\mathbf{q}-\mathbf{k})\cdot\xi_s(t). \qquad (3)$$

Equations (2) and (3) embody the *instantaneous frequency* and *instantaneous phase*, within the concept of angle modulation. The propagation medium constitutes the "communication channel" while the surface vibration assumes the role of the modulator. In the case of ultrasonic sensors, assuming plane waves, the received pressure field is:

$$p_r(r,t) = |p_r| e^{i\mathbf{q}\cdot\mathbf{r}} e^{-i\left[\omega_i t + (\mathbf{q}-\mathbf{k})\cdot\mathbf{n}_s \frac{u_s}{\Omega}\sin\Omega t\right]}, \qquad (4)$$

where $|p_r|$ is its magnitude. The right-hand exponent term in the brackets represents a sinusoidal modulation of the signal phase. Frequency or phase demodulation of the received signal generates a voltage proportional to the instantaneous frequency $\omega_i(t)$ or phase $\Phi_r(t)$, respectively,[28] and thus retrieves the vibration information. Although the two types of angle modulation are mathematically inseparable, a fine line is drawn between them within the context of practical vibrometer design. Equations (2) and (3) state that frequency demodulation yields a direct measure of the vibration *velocity* amplitude, while phase demodulation is directly related to the *displacement* amplitude. If the medium has sizable acoustic nonlinearities, the phase in Equation (3) is supplemented by nonlinear mixing terms.

In keeping with electronic communications nomenclature, a *phase modulation index* is introduced as

$$\beta \equiv (\mathbf{q}-\mathbf{k})\cdot\mathbf{n}_s \frac{u_s}{\Omega}. \qquad (5)$$

For ultrasonic sensors, assuming $u_s << c_0$ (c_0 being the speed of sound in the medium), β becomes[29]

$$\beta \approx \frac{2\omega_i}{c_0}\frac{u_s}{\Omega}\cos\theta = \frac{2\omega_i}{c_0}\xi_s\cos\theta . \qquad (6)$$

$\xi_s \equiv u_s/\Omega$ denotes the displacement amplitude and θ is the incidence angle, as in Figure 1. The presence of the surface vibration angular frequency Ω in the denominator indicates an analogy to narrowband angle modulation by a single tone, corresponding to weak modulation amplitudes. Using the generating function for Bessel functions as $e^{iz\sin\theta} = \sum_{n=-\infty}^{\infty} J_n(z)e^{in\theta}$, Equation (4) becomes

$$p_r(r,t) = \sum_{n=-\infty}^{\infty} |p_r| J_n(\beta) e^{-i(\omega_i + n\Omega)t} e^{iq\cdot r} , \qquad (7)$$

where J_n is the Bessel function of the first kind. Equation (7) is essential to investigating the operation of ultrasonic vibrometers. The energy in the received ultrasonic field is divided between the central "carrier" (n = 0) and an infinite number of symmetric sidebands, of frequencies $\omega_i \pm n\Omega$ and amplitudes $|p_r| J_n(\beta)$. In the world of electronic communications, this is typical of angle modulation: the PM (or FM) sidebands siphon energy out of the primary (carrier) signal. The sidebands contain all the information pertinent to the surface vibration. Taking the analogy to electronic communications further, it is conceivable to think about the possibility of increasing the modulation index up to the first zero of J_0, that is $\beta = 2.405$, in which case the detected carrier amplitude is virtually zero and all the energy is transferred into the sidebands. However, for practical purposes, this corresponds to an increase of, say, the surface displacement amplitude by several orders of magnitude.

For very small modulation indices, the only surviving orders in the Bessel series are n = 0, ±1; this is equivalent to the received signal having a bandwidth of approximately Ω/π. The Bessel functions

satisfy $J_{-1}(\beta) = -J_1(\beta)$ and, given the small-argument behavior of Bessel functions, $J_0(\beta) \approx 1$ and $J_1(\beta) \approx \beta/2$. Thus the vibration sidebands are out of phase, with amplitudes (called *SB*, for simplicity) given by

$$SB \approx \pm |p_r| \frac{u_s}{\Omega} \frac{\omega_i}{c_0} \cos\theta . \qquad (8)$$

Assuming weak dissipation, the magnitude of the received pressure is close to that of the incident field, $|p_r| \approx |p_i|$. Equations (6)–(8) are central to understanding the sensitivity issues of ultrasonic vibration sensors. It is clear that the sensitivity can be increased if i) the vibration displacement (or velocity) amplitude is increased, ii) the probe frequency is larger or iii) the probe strength is increased. A local reduction of the sound speed will also lead to increased detection sensitivity; this could be attained, *e.g.* by enclosing the sensor head into a "bubble" containing a "slow" medium, in contact with the probed surface. However, such an approach may give rise to problems associated to standing-waves, losses etc., which have to be investigated further.

Any relative motion between the sensor head and the surface generates additional Doppler peaks which may lie inside the measurement bandwidth. In addition, sensor oscillations, whether coherent with the surface vibrations or due to nearby equipment, will affect operation. Piquette and Van Buren address this scenario in the context of underwater vibration sensing. Proper vibration insulation along with a judicious choice of scanning speed will help alleviate these factors. An interesting technique for factoring out any additional target-sensor relative motion developed for laser vibrometry is explained in detail in Ref. 30.

III. SIGNAL DEGRADATION

The spectral purity of the measurement signals is perhaps the most basic requirement of sensor development. In many cases, quadrature Doppler systems suffer from imbalances in amplitude and

phase.[31] These may result in signals larger than the measured vibration levels; if they are close to the vibration frequencies, they can introduce sizable errors in the demodulation process.

In addition to electronic noise incurred in detection, a major source of signal degradation for an air-coupled acoustic sensor is vortical or turbulent air motion (*e.g.* vortex shedding induced by sensor motion or wind). By analogy with electronic communications it can be said that the role of wind is that of "channel noise" (albeit not "white", but intermittent). As the speed of air motion increases, the sensor detects a progressively richer (turbulent) spectrum that can ultimately overwhelm the information-bearing sidebands. Many authors have developed models aimed at quantifying acoustic scattering in turbulent media.[32,33] The far-field expression for the scattered acoustic pressure per unit volume derived in Ref. 33 is easily amenable to experiments. The scattering mechanism can be described qualitatively as follows: eddies with specific length scales, excited by the incident field of frequency $\omega_i/2\pi$ on time scales smaller than the typical turbulent time scales, become acoustic sources radiating at different frequencies $\omega/2\pi$. Contreras and Lund[34] arrived at an equivalent expression for scattering by thermal turbulence. Various authors[35,36,37] have done intensive experimental studies of ultrasound scattering by turbulence.

Additionally, wind blowing over grass-covered surfaces induces a complex multi-component motion of the grass blades, which is detected by the vibrometer. Common laser vibrometers relying on back-scattered light tend to be susceptible to this phenomenon: in-plane motion of a grass blade randomly alters the spatial characteristics of the speckle pattern inherent in coherent scattering from surface irregularities on the order of the optical wavelength. This, in turn, causes significant drops in the demodulated signal.[38,39] In the ultrasonic case, the noticeably larger "acoustic speckle" precludes any such tendencies. Fiber-coupled laser Doppler sensors are also affected by fiber vibrations induced by wind or other sources. A very clear and systematic theoretical/experimental investigation of environmental effects on fiber-coupled systems is given in Ref. 40.

In the absence of wind, signal degradation also appears as a result of scattering of the incident field from surface inhomogeneities (grains, pebbles etc.) and rooted or loose vegetation (grass, fallen leaves, pine needles, moss etc.) with characteristic length scales. Conceptually, this type of scattering is expected to impose lesser constraints on acoustic sensors due to the relative ease of transducer tunability. However, decreasing the probe frequencies in order to "see through" various scattering agents comes at the price of reduced Doppler sensitivity (Equations (6) and (8)).

IV. EXPERIMENT, RESULTS AND DISCUSSIONS

The experimental arrangement is shown in Figure 1. Two similar custom-made piezoelectric transducers (center frequency $\approx$ 120 kHz, bandwidth $\approx$ 10 kHz, total divergence $\approx 9^{o}$) acting as transmitter (TX) and receiver (RX) form the sensor. The angle between each transducer axis and the normal is 13^{o}; the average sensor elevation was 14 cm, resulting in a total path length (transmitter to receiver) of 28 cm. The modulated carrier is filtered and amplified by a low-noise preamplifier (SR560) and subsequently fed to a HP89410A vector signal analyzer (VSA), capable of real-time demodulation. An HP8904A signal generator supplies the transducer excitation for most measurements. Commercial shakers are used to excite the vibration of the probed surface. Two types of shakers are used: a clamped-plate type (AURA model AST-2B-4, f_{res} = 40 Hz) and a piston type (LDS model V203, broadband). The surface displacement amplitude is monitored with a Polytec PDV 100 laser Doppler vibrometer (LDV). In the next sections, the acronym UDV will be used for ultrasonic Doppler vibrometry. V_{TX} is the voltage applied to the ultrasonic transmitter, proportional to the incident pressure magnitude. This choice is warranted by the fact that absolute, quantitative measurements are not the primary goal of the present study. The vibration levels are low enough so that the linear regime holds and only the 1st order sidebands are observed.

A. Energy balance

A typical spectrum of the Doppler signal received from an Al plate attached rigidly to an LDS shaker is shown in Figure 2. The received acoustic energy is split between the carrier and the sidebands. Increasing the vibration level leads to an increase of the sideband amplitude accompanied by a mild decrease in the carrier amplitude. The importance of this interplay is didactic in that it embodies a core principle of Doppler vibrometry. Moreover, ultrasonic vibrometers enable one to look directly at *both* the carrier and the sidebands; in the optical case, one must down-convert the carrier frequency by many orders of magnitude before even attempting to monitor it. In the present configuration, for the relatively low transmitter excitation used (<1W), the minimum displacement detected was approximately 200 nm without averaging and 25 nm with averaging; these figures can be improved if larger drive levels are used. Lower excitation levels were preferred in order to preclude sensor saturation effects.

B. Measurements on a sand surface

The aim of this investigation is to assess the ability of an ultrasonic sensor to follow the output of a commercial laser Doppler vibrometer, in a more realistic scenario. The AURA shaker, excited at 150 Hz, was buried in sand; the probe frequency was 120.4 kHz. The vibrations of the surface above the shaker were probed in parallel with the UDV and the LDV (the latter was aimed at an incidence angle $\theta_{LDV} = 17.5^{o}$. The results are shown in Figure 3. The data set in case (a) corresponds to the shaker surface being flush with that of the sand. Cases (b) and (c) were taken with the shaker buried approximately 2.5 cm beneath the surface, one day apart from each other. The upper plots show the sideband amplitude together with the point-wise surface displacement measured with the LDV, for increasing shaker excitation, V_S. The energy dynamics between the carrier and the sidebands is evident in the lower graphs showing the carrier behavior. The vibration information obtained ultrasonically has a structure similar to that obtained with the LDV. As an aside, it is interesting to note the behavior of the sand surface during the process. The UDV/LDV vibration response is not linear; nor should one expect it to be (e.g. complex sand response to low-frequency excitation, inertial effects on shaker operation due

to a non-rigid base etc). Moreover, the sideband and carrier amplitudes have an interesting interplay in all three cases. Case (c) is unarguably the most intriguing: the onset of the "vibration saturation" regime at $V_S \approx 2.5$ V (apparent in both UDV and LDV data) may indicate a particular dynamic state of the grains between the shaker and the surface. In all three cases, it is possible that a correlation exists between the carrier curve and the local slope of the sideband curve. These issues remain open to further investigation.

C. The influence of air motion and surface vegetation

Surface scattering centers as well as wind affect both laser and ultrasonic Doppler vibrometers. The scattering strength depends primarily upon the wavelength-to-obstacle-dimension ratio. This ratio is more easily controllable for an UDV than it is for an LDV. Simple experiments have been performed in order to assess the influence of various scenarios involving surface scatterers and ambient air motion. One case involves scattering from a bed of randomly oriented pine needles strewn on top of the shaker plate (f_{probe} = 120.4 kHz, $f_{surface}$ = 150 Hz). The average width of the pine needles is 1.5 mm, which represents an approximate fraction of 0.52 of the ultrasonic probe wavelength. Figure 4 shows waterfall displays of real-time LDV and UDV demodulated spectra. $\Phi_{UDV}(\omega)$ is the FFT of the demodulated phase of the ultrasonic signal. The time index entries represent times separated by about 0.33 s. The UDV signal keeps a fairly constant signal-to-noise ratio (SNR) over significantly longer time spans than the LDV does. The plots in Figure 5 show time-averages of such data.

In order to study the combined effects of wind and surface vegetation, a "rooted-grass simulator" was built from 4mm wide paper strips with an average length of 30 mm inserted in a closed-cell foam substrate. The average "grass" density was approximately 1.77 blades / cm^2. The "grass simulator" was placed on the shaker plate. To be able to get a definite assessment, the shaker displacement was deliberately set to a relatively high value (approx. 550 nm). A relatively weak jet of nitrogen was used to set the "grass" blades in oscillatory motion, independent of the surface vibration. The jet was positioned as close to the foam surface as possible. The LDV beam was focused on a moving blade that was also

inside the ultrasonic spot size. Figure 6 shows explicitly an instance where the LDV signal is completely overwhelmed, while the UDV still produces a useful output. A major component of the unsteady motion of the "grass" blades is indicated by the closest satellite peak structure around the carrier. The onset of "grass" motion is discussed in more detail next.

A series of measurements was performed with the UDV in order to separate out the effects of the "wind structure" itself and that of the grass motion. Three data sets were taken with the jet entering the sensing region at three different heigl c) ıe heights were chosen such that the air motion interacts gradually with the grass. Figure 7 shows the UDV signal as the jet is lowered from a condition of virtually no grass motion (a) to relatively strong grass motion (c); the 150 Hz vibration sidebands are clearly seen. In case (a), only the jet "structure" (e.g. eddies) scatters the acoustic field. In (b), the jet barely "touches" the tips of the "grass" blades, setting some of them in unsteady motion (as observed by visual inspection). In this case, the overall shape of the turbulent Doppler "hump" is similar to that from case (a), with the exception of the incipient structure at approximately 17 Hz to the right and left of the carrier frequency. This can be explained by the fact that the vorticity field has a greater effect than the blade motion. The satellite structure develops as the jet is lowered further, to case (c), when it hits the blades "head-on" and sets a large number of them in motion. This time, the spectrum differs more visibly from that of (a); the pronounced peaks around the carrier indicate the onset of jet-induced grass vibrations. A similar structure appears in the lower plot of Figure 6a.

Note. Choosing jets in order to deconstruct the effects of wind may seem a naive choice; yet it is not so far-fetched: although the structure of the wind close to the ground is the subject of continuous debate, it is believed to have a Kolmogorov spectrum, characterized by eddies of many length scales.[41] The turbulent scattering mechanism depends on the relationship between the incident wavelength and eddy size. The very fact that the jet influences the ultrasonic field as seen in Figure 7 indicates that there exist eddy scales commensurate with the probe wavelength.

V. CONCLUSIONS

A number of topics pertinent to the use of air-coupled ultrasound to probe ground vibrations have been discussed. It has been shown that the operation of a UDV system can be adequately described by the frequency or phase modulation: part of the energy of the incident field is transferred from the carrier to the information-bearing sidebands. On a non-rigid, granular surface (sand), the performance of the UDV prototype is comparable to that of a commercial LDV. Moving one step further, to the scenario of vegetation-covered surfaces, it has been shown that a moving pine needle or a grass blade may be the Achilles' heel of optical sensors due to speckle-induced signal loss. Of course, a UDV is expected to experience similar difficulties when the scatterers become greater than the wavelength. Investigation of "grass blade dynamics" may prove useful in understanding these effects. For instance, studies of i) flexural (and other) modes excited in the blade as a result of periodic forcing applied at its root and ii) complex vibrational modes excited by unsteady air motion, will be useful.

Another intriguing aspect is the behavior of the ultrasonic Doppler sensor in the presence of wind. However detrimental wind can be in the detection of small vibrations, it nevertheless brings a whole new dimension into the problem: that of scattering by turbulence. The better one understands its mechanism, the more likely one is to develop reliable techniques for wind alleviation in air-coupled acoustic vibrometry. Passive wind noise reduction may be as simple as using a shield around the sensing volume. An alternative option consists of the "homogenization" of the air turbulence by making the shield walls out of reticulated materials; the choice of the "cell" size is dictated, for example, by the requirement that the average eddy size be smaller than the ultrasonic wavelength, to inhibit scattering. Active techniques may involve ways to manipulate the received wind spectrum. If an absorption line at the vibration frequency could be burned into the turbulent spectrum detected by the UDV, then the SNR could be improved locally, at the vibration sidebands.

ACKNOWLEDGMENTS

The authors extend their gratitude to Prof. Christoffe Baudet, Roger Waxler, Barton Smith, and Ning Xiang, for fruitful discussions. The work is supported by a grant from the Office of Naval Research.

REFERENCES

1. J. M. Sabatier, H. E. Bass, L. E. Bolen, and K. Attenborough "Acoustically induced seismic waves", J. Acoust. Soc. Am. **80** (2), 646-649 (1986).

2. J. M. Sabatier, H. E. Bass, and G. R. Elliott, "On the location of frequencies of maximum acoustic-to-seismic coupling", J. Acoust. Soc. Am. **80** (4), 1200-1202.

3. K. Attenborough, H. E. Bass, and J. M. Sabatier, "Elastic properties of the Earth's surface", Chapter 15 in *Handbook of Elastic Properties of Solids, Liquids, and Gases, vol. III: Elastic Properties of Solids: Biological and Organic Materials, Earth and Marine Sciences*, edited by Levy, Bass and Stern, Academic Press, 2001.

4. W. Patrick Arnott and J. M. Sabatier, "Laser-Doppler vibrometer measurements of acoustic to seismic coupling", Appl. Acoust. **30**, 279-291 (1990).

5. N. Xiang and J. Sabatier, "Pre-differentiated M-sequences for laser-Doppler-based identification of vibrational systems", J. Acoust. Soc. Am. **106** (2), 2215 (A) (1999).

6. J. M. Sabatier and N. Xiang, "Laser-Doppler-based acoustic-to-seismic detection of buried mines", Proc. SPIE. **3710**, 215-222 (1999).

7. C. J. Hickey, J. M. Sabatier and T. M. McGee, "A method for the detection of shallow buried objects", Annali Di Geofisica, **43** (6), 1225-1233.

8. W. R. Scott, Jr., C. Schroeder, and J. S. Martin, "An acousto-electromagnetic sensor for locating land mines", Proc. SPIE **3392**, *Detection and Remediation Technologies for Mines and Minelike Targets III*, 176-186, April 1998

9. J. S. Martin et al., "Ultrasonic displacement sensor for the seismic detection of buried landmines", Proc. SPIE: 2002 Annual International Symposium on Aerospace/Defense Sensing, Simulation and Controls, Orlando, FL, April 2002.

10. C. T. Schroeder and W. R. Scott, Jr., "On the complex conjugate roots of the Rayleigh equation: The leaky surface wave", J. Acoust. Soc. Am. **110** (6), 2867-2877 (2001).

11. H. Russer and V. Magori, "Phase coincidence between ultrasound and microwaves – a powerful and flexible multisensor principle", Eurosensors XIV, 28-30 August 2000, Copenhagen, Denmark.

12. H. Russer and V. Magori, "Sweep linearization of a microwave FMCW Doppler sensor by an ultrasonic reference", IEEE Intern. Freq. Control Symp., 201-206, Orlando, Fl, 1997.

13. K. Naugolnykh and L. Ostrovsky, *Nonlinear Wave Processes in Acoustics*, Chapter 5, Cambridge, 1998.

14. O. Casula and D. Royer, "Transient surface velocity measurements in a liquid by an active ultrasonic probe", IEEE Trans. Ultrason. Ferroel. Freq. Control, **45** (3), 760-767 (1998).

15. D. Royer and O. Casula, "A sensitive ultrasonic method for measuring transient motions of a surface", Appl. Phys. Lett. **67** (22), 1706-1715 (2001).

16. C. Barriere and D. Royer, "Diffraction effects in the parametric interaction of acoustic waves: application to measurements of the nonlinearity parameter B/A in liquids", IEEE Trans. Ultrason. Ferroel. Freq. Control, **48** (6), 760-767 (1998).

17 . M. Cox and P. H. Rogers, "Ultrasonic measurements of the vibrational amplitudes of auditory organs in fish", Advances in Test and Measurement **23**, 337-350 (1986).

18. S.-R. Huang, R. M. Lerner, and K. J. Parker, "On estimating the amplitude of harmonic vibration from the Doppler spectrum of reflected signals", J. Acoust. Soc. Am. **88**, 2702-2712 (1990).

19. S.-R. Huang, R. M. Lerner, and K. J. Parker, "Time domain Doppler estimators of the amplitude of vibrating targets", J. Acoust. Soc. Am. **91**, 965-974 (1992).

20. P. H.. Rogers and M. Cox, Noninvasive Vibration Measurement System, U. S. Patent No. 4,819,649, April 11, 1989.

21. D. Censor, "Harmonic and transient scattering from time-varying obstacles", J. Acoust. Soc. Am. **76** 1527-1534 (1984).

22. D. Censor, "Scattering by time-varying obstacles", J. Sound Vib. **25**, 101-110 (1972).

23. D. Censor, "Acoustical Doppler effect analysis – Is it a valid method?", J. Acoust. Soc. Am. **83**, 1223-1230 (1988).

24. J. C. Piquette and A. L. Van Buren, "Comments on 'Harmonic and transient scattering from time-varying obstacles' ", J. Acoust. Soc. Am. **76**, 1527-1534 (1984).

25. J. C. Piquette and A. L. Van Buren, "Some further remarks regarding scattering of an acoustic wave by a vibrating surface ", J. Acoust. Soc. Am. **80**, 1533-1536 (1986).

26. J. C. Piquette and A. L. Van Buren, "Nonlinear scattering of acoustic waves by vibrating surfaces ", J. Acoust. Soc. Am. **76**, 880-889 (1984).

27. J. D. Jackson, *Classical Electrodynamics*, 2nd Edition, Wiley, New York, 1975.

28. B. P. Lathi, *Modern Digital and Analog Communication Systems*, Ch. 5, Oxford University, New York, 1998.

29. A. D. Pierce, Acoustics. *An Introduction to Its Physical Principles and Applications*, p.456, McGraw-Hill, New York, 1981.

30. A. Hocknell, R. Jones, and S. J. Rothberg, "Remote vibration measurements: compensation of waveform distortion due to whole body translations", J. Sound and Vib. **214** (2), 285-307 (1998).

31. R. Moraes and D. H. Evans, "Compensation for phase and amplitude imbalance in quadrature Doppler signals", Ultrasound in Med. and Biol., **22** (1), 129-137 (1996).

32. R. H. Kraichnan, "The scattering of sound in a turbulent medium", J. Acoust. Soc. Am. **25**, 1096-1104, (1953).

33. F. Lund and C. Rojas, "Ultrasound as probe of turbulence", Physica D **37**, 508-514 (1998).

34. H. Contreras and F. Lund, "Ultrasound as a probe for turbulence II, Temperature inhomogeneities", Phys. Lett. **149**, 127-130 (1990).

35. N. Schaeffer, "Diffusion d'ultrasons: Mesures dans un jet d'air turbulent" (Ultrasonic scattering: Measurements in a turbulent air jet), M.Sc. Thesis, École Normale Supérieure de Lyon, Lyon, France (2001).

36. C. Baudet, S. Ciliberto, and J. F. Pinton, "Spectral analysis of the von Karman flow using ultrasound scattering", Phys. Rev. Lett. **67** (2), 193-195, (1991).

37. C. Baudet, O. Michel, and W. J. Williams, "Detection of coherent vorticity structures using time-scale resolved acoustic spectroscopy", Physica D **128**, 1-17 (1999).

38. C. B. Scruby and L. E. Drain, *Laser Ultrasonics. Techniques and Applications*, 89-97, Adam Hilger, Bristol, 1990.

39. S. J. Rothberg, J. R. Baker, and N. A. Halliwell, "Laser vibrometry: pseudo-vibrations", J. Sound and Vib. **135**, 516-522 (1989).

40. C. N. Pannell, J. D. C. Jones, and D. A. Jackson, "The effect of environmental acoustic noise on optical fibre based velocity and vibration sensor systems", Meas. Sci. Technol. **5**, 412-417 (1994).

41. R. B. Stull, *An Introduction to Boundary Layer Meteorology,* 390-393, Kluwer Academic, 2001.